ISSN 1674-1056
http://cpb.iphy.ac.cn
http://iopscience.iop.org/cpb
中国物理 B
Chinese Physics
中国物理
Chinese Physics B

The influence of surface effects on Frederiks transition in nematic liquid crystal doped with ferroelectric nanoparticles

Erfan Kadivar, Mojtaba Farrokhbin
Citation: Chin. Phys. B . 2018, 27(4): 046801. **doi:** 10.1088/1674-1056/27/4/046801

Journal homepage: http://cpb.iphy.ac.cn; http://iopscience.iop.org/cpb

What follows is a list of articles you may be interested in

Thermo-controllable self-assembled structures of single-layer 4, 4"-diamino-p-terphenyl molecules on Au (110)

Junhai Ren(任俊海), Deliang Bao(包德亮), Li Dong(董立), Lei Gao(高蕾), Rongting Wu(武荣庭), Linghao Yan(闫凌昊), Aiwei Wang(王爱伟), Jiahao Yan(严佳浩), Yeliang Wang(王业亮), Shixuan Du(杜世萱), Qing Huan(郇庆), Hongjun Gao(高鸿钧)
Chin. Phys. B . 2017, 26(8): 086801. **doi:** 10.1088/1674-1056/26/8/086801

Phase transition and critical behavior ofspin-orbital coupled spinel ZnV_2O_4

Li Wang(王理), Rong-juan Wang(王蓉娟), Yuan-yuan Zhu(朱媛媛), Zhi-hong Lu(卢志红),Rui Xiong(熊锐), Yong Liu(刘雍), Jing Shi(石兢)
Chin. Phys. B . 2016, 25(1): 016802. **doi:** 10.1088/1674-1056/25/1/016802

Phase behaviors of binary mixtures composed of banana-shaped and calamitic mesogens

M. Cvetinov, D. Ž. Obadović, M. Stojanović, A. Vajda, K. Fodor-Csorba, N. Eber, I. Ristić
Chin. Phys. B . 2014, 23(9): 096402. **doi:** 10.1088/1674-1056/23/9/096402

An effective-field theory study of hexagonal Ising nanowire：Thermal and magnetic properties

Yusuf Kocakaplan, Ersin Kantar
Chin. Phys. B . 2014, 23(4): 046801. **doi:** 10.1088/1674-1056/23/4/046801

The influence of surface effects on Frederiks transition in nematic liquid crystal doped with ferroelectric nanoparticles

Erfan Kadivar[1,†] and Mojtaba Farrokhbin[2,‡]

[1] *Department of Physics, Shiraz University of Technology, Shiraz* 71555-313, *Iran*
[2] *Department of Physics, Faculty of Sciences, Yazd University, Yazd* 89195-741, *Iran*

(Received 11 November 2017; revised manuscript received 3 January 2018; published online 29 March 2018)

Motivated by our recent work, in this work, we present the numerical study of the anchoring effect on the Frederiks threshold field in a nematic liquid crystal doped with ferroelectric colloidal nanoparticles. Assuming weak anchoring conditions, we employ the relaxation method and Maxwell construction to numerically solve the Euler–Lagrangian differential equation for the total free energy together the Rapini–Papoular surface energy to take into account anchoring of nematic liquid crystal molecules at the substrates. In this study, we focus our attention on obtaining the phase diagrams of Frederiks transition for different values of anchoring strength which have been not computed in our previous work. In this way, the effect of nanoparticle radius, nanoparticle volume fraction, nanoparticle polarization, and cell thickness on the Frederiks transition for different values of anchoring conditions are summarized in the phase diagrams. The numerical results show that by increasing the nanoparticles size and nanoparticle volume fraction in the ferronematic system, the Frederiks threshold field is strongly reduced.

Keywords: anchoring surface effect, ferronematics, Frederiks transition, Maxwell construction

PACS: 68.35.Rh, 77.84.Nh, 64.70.M–, 05.70.Np **DOI:** 10.1088/1674-1056/27/4/046801

1. Introduction

During the last few years, liquid crystals (LCs) with extraordinary optical properties are widely used at many optical devices as the spatial light modulators[1–6] and photorefractive cells,[7–9] which provide modulation, diffraction, and polarization of light.[10–12] Because of LCs dielectric and diamagnetic features, their optical properties will be easily controlled by applying electric or magnetic field. A suspension of ferroelectric nanoparticles (NPs) embedded in nematic liquid crystal (NLC) matrix is known as ferronematic system. The ferronematic research field was first opened by a key paper[13] and the key early theoretical works in this field are provided by Raikher.[14–17] The application of ferroelectric nanomaterials in liquid crystals has recently emerged as a promising way for advanced and tunable electro-optical materials in experimental work.[18]

Several advantages in combing the NPs and LCs materials have been appeared through manipulation their fluidity, unique anisotropic and elastic constants by which its switchable matrix will be promoted. Moreover, NPs which possess both shape and dielectric anisotropy transfer self-organization in the LC medium and by this way, modify[19] and/or produce[20] new features not available by either materials in their intrinsic form. The small ferroelectric colloidal particles are chosen as the impurity and have a length scale of nanometer by which they are not able to disrupt NLC host and also not able to form periodic array done in photonics application.[21–26] However, a low concentration of ferroelectric NPs into the NP-NLC hybrid systems causes significant properties.[27–32] For example, the Kerr effect, isotropic-nematic transition temperature and orientational order parameter will be increased. While, transition threshold field will be decreased. Mukherjee used Landau phenomenological theory to study the effects of ferroelectric nanoparticles on the static dielectric permittivity[33] and Kerr effect.[34]

Surface alignment play a key impact on determining the electro–optical properties of LC-based devices.[35] The LC cell surfaces coated with aligning agent impose a preferred LC molecular orientation at the wall, refereed to as anchoring. Here, NP-NLC hybrid system is supposed to possess a homogeneous anchoring condition by which the NLC molecules are oriented parallel to the substrate. There are two limiting cases for the surface anchoring: strong and weak anchoring conditions. The weak anchoring of NLC can in principle result in lower threshold field. From practical point of view, there are several surface modification techniques to achieve weak anchoring configuration at the slab wall such as Mechanical rubbing,[36,37] photo alignment,[38] surface polarization,[39] wetting phenomenon,[40,41] self-assembled monolayers,[42] grafting of polymer brushes,[43] and atomic force microscope treated surfaces.[44]

In this study, we have numerically investigated the effects of anchoring energy on the Frederiks threshold field in a nematic liquid crystal doped with ferroelectric colloidal nanopar-

†Corresponding author. E-mail: erfan.kadivar@sutech.ac.ir
‡E-mail: m.farrokhbin@gmail.com

© 2018 Chinese Physical Society and IOP Publishing Ltd

ticles. A key input to the present work comes from our previous work,[45] in which NLC director configuration within the ferronematic cell has been studied through strong anchoring conditions. At weak anchoring conditions, nanoparticle volume fraction, nanoparticle size, nanoparticle polarization, and cell thickness have a key role in the Frederiks transition. However, these effects have been not discussed in previous work. In this work, we will obtain a phase diagram for nanoparticle radius, volume fraction, polarization and also slab thickness for different values of anchoring strength which have been not investigated in our previous work. To fulfill this task, we suppose a simplified model to tackle some complexities arisen out of weak anchoring condition. So, we assume the following postulates: (i) to avoid fully disruption NLC properties, sufficiently low concentration and sample size of ferroelectric NPs are chosen; (ii) NPs permanent polarization can be either parallel or anti-parallel to the NLC director; (iii) induced electric field by NP polarization is neglected; and (iv) NP-NP interactions will not taken into account here.

2. Physical model

We consider a suspension of ferroelectric colloidal NP embedded in NLC medium, refereed to as ferronematic system. This cell is confined between two parallel substrates fixed at $z = 0$ and $z = L$. We also suppose homogeneous alignment layers coated on the substrates. Therefore, NLC molecules at the interface are oriented parallel to the substrate. Cell geometry is schematically depicted in Fig. 1. As shown in Fig. 1, an external electric field $\boldsymbol{E} = (0,0,E)$ is applied along the z axis, perpendicular to the substrates. Angle θ is defined between x axis and $\hat{\boldsymbol{n}}$ direction. Polarization of ferroelectric NPs causes drastic effects in comparison to the pure NLC medium and hence results in interesting features. For simplicity, we only suppose ferroelectric NP has a spherical shape, permanent polarization, d, and totally occupies, f, fraction of the total volume.

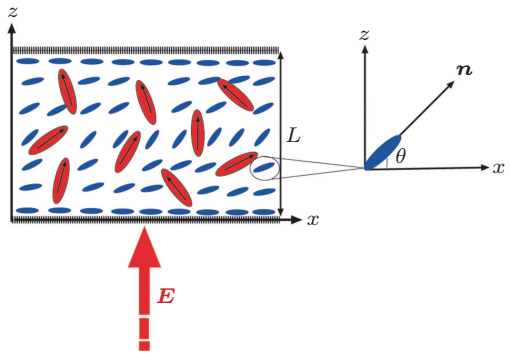


Fig. 1. (color online) Shematic representation of a ferronematic cell consisting of nematic liquid crystal (NLC) doped with ferroelectric NPs. In field-off state, homogeneous alignment layers at the substrates cause NLC molecules to be directed parallel to the interfaces and NPs electrostatic dipole moments are randomly distributed. θ is defined as the angle between nematic director and x axis, $\boldsymbol{n} = (\cos\theta(z), 0, \sin\theta(z))$.

A bulk free energy function to describe the suspension of ferroelectric NPs embedded in NLC system was first provided by Raikher.[14–17] The bulk free energy density based on the continuum theory can be written in terms of elastic, electric, entropy, and surface energies:

$$f = f_{\rm el} + f_E + f_{\rm entr} + f_{\rm surf}, \tag{1}$$

where

$$f_{\rm el} = \frac{1}{2}\left\{K_1(\nabla\cdot\boldsymbol{n})^2 + K_2(\boldsymbol{n}\cdot(\nabla\times\boldsymbol{n}))^2 + K_3(\boldsymbol{n}\times(\nabla\times\boldsymbol{n}))^2\right\},$$
$$f_E = -\frac{1}{2}\boldsymbol{D}_0\cdot\boldsymbol{E} - \boldsymbol{P}\cdot\boldsymbol{E}_0, \quad f_{\rm entr} = f\frac{k_{\rm B}T}{v}\left(\rho_+\ln\rho_+ + \rho_-\ln\rho_-\right), \tag{2}$$

where K_1, K_2, and K_3 are splay, twist, and bend Frank elastic modules of NLC, respectively. ρ_+ and ρ_- stand for fraction of ferroelectric NP oriented parallel or antiparallel to the local director field, $\boldsymbol{P}$ is the permanent polarization of the colloidal NP per unit volume, $\boldsymbol{D}_0$ is the electric displacement arisen out of only NLC characterization, and $\boldsymbol{E}_0 = \lambda\boldsymbol{E}$ is electric field inside the cell.

In this paper, we use the anchoring of the molecules to the bounding surfaces, which is quantified by Rapini–Papoular free energy density[46]

$$f_{\rm s} = \frac{1}{2}A\sin^2\theta_0, \tag{3}$$

where A is the anchoring strength, θ_0 is the angle between easy direction and the nematic director at the nematic-wall interfaces, $\theta(z=0) = \theta(z=L) = \theta_0$. Thus, the total density free energy of nematic liquid crystal doped with ferroelectric nanoparticles reads as follows:[45]

$$f = \frac{1}{2}\left(K_1\cos^2\theta + K_3\sin^2\theta\right)\left(\frac{{\rm d}\theta(z)}{{\rm d}z}\right)^2 - \frac{1}{2}\varepsilon_0\left(\varepsilon_\perp + \varepsilon_a\sin^2\theta\right)E_z^2(\theta)$$
$$- \frac{f}{\beta v}\ln\left[\exp\left(\lambda d v\beta E_z(\theta)\sin\theta\right) + \exp\left(-\lambda d v\beta E_z(\theta)\sin\theta\right)\right] + \frac{1}{2}A\sin^2\theta_0, \tag{4}$$

where v is the nanoparticle volume, $\beta = 1/k_B T$, and $\varepsilon_a = \varepsilon_{\parallel} - \varepsilon_{\perp}$ is an anisotropy of dielectric susceptibility.

Variation in the total free energy in order to determine the equilibrium orientation $\theta(z)$ that minimizes the total free energy leads to the following Euler–Lagrange differential equation:

$$\frac{\mathrm{d}^2\theta(z)}{\mathrm{d}z^2} = \frac{\left[(K_1 - K_3)\,\theta'^2 - \varepsilon_0\varepsilon_a E_z^2(\theta)\right]\sin\theta\cos\theta - f\lambda d E_z(\theta)\cos\theta\tanh\left(\lambda d v\beta E_z(\theta)\sin\theta\right)}{K_1\cos\theta} + K_3\sin^2\theta, \tag{5}$$

together with two boundary conditions at the interfaces,

$$\theta(z=0) = \theta(z=L) = \theta_0 \tag{6}$$

and

$$\left.\frac{\mathrm{d}\theta}{\mathrm{d}z}\right|_{z=0,L} = \pm\frac{(1/2A)\sin(2\theta_0)}{K_1\cos^2\theta_0 + K_3\sin^2\theta 0}, \tag{7}$$

where plus and minus signs refer to the boundary conditions at $z = 0$ and $z = L$, respectively.

Differential equation (5) is solved numerically by using the relaxation method for arbitrary values of θ_0. Once $\theta(z)$ profile for each value of θ_0 is obtained, we plot $\left.\frac{\mathrm{d}\theta}{\mathrm{d}z}\right|_{z=0}$ as a function of θ_0. According to Eq. (7), the possible solutions of θ_0 are intersections with the right side of Eq. (7). Figure 2 shows a graphical solution of Eq. (7). Cross and circle points are refereed to the right and left sides of Eq. (7), respectively. There are three periodic solutions at $[0, \pi]$ interval. Nevertheless, from physical point of view, the only acceptable solution is the one which turns the total free energy to the absolute minimum value. The physically acceptable solution is selected by using well-known Maxwell construction.[45,47]

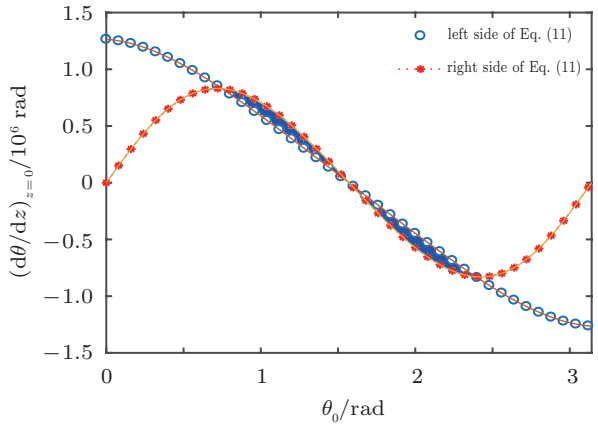


Fig. 2. (color online) Graphical solution of Eq. (5) with the boundary conditions of Eq. (7) under the influence of applied electric field $E = 3.95\times10^5$ N·C^{-1}, anchoring strength $A = 2\times10^{-5}$ J·m^{-2}, NP volume fraction $f = 0.3\%$, NPs' permanent polarization $d = 0.06$ C·m^{-2}. Cross points and circle points are related to the right and left sides of Eq. (7). Right and left sides of Eq. (7) intersect at three places in the interval $[0, \pi]$. The striking feature is that x_2 always locates in $\pi/2$ radians and provides the maximum total free energy. While, x_1 and x_3 are 0.7486 and 2.3930 in our considered parameters for this ferronematic system, respectively. Increasing applied electric field strength results in gradually shifting the current value of x_1 to its final value $\pi/2$ radians which means all molecules will be directed along the applied field. However, x_1 and x_3 differ $\pi/2$ from each other. This feature comes from the fact that $\boldsymbol{n}$ and $-\boldsymbol{n}$ are equivalent in NLC systems. Since area 1 is larger than area 2, x_1 is the only acceptable physical solution here and gives the absolute minimum of the total free energy.

To find the Frederiks threshold field, we increase the applied electric field strength from zero. Below Frederiks transition, orientation of NLC molecules or director $\hat{\boldsymbol{n}}$ does not change. However, as the applied electric field strength reaches to the Frederiks field, director $\hat{\boldsymbol{n}}$ and thus θ_0 starts to tilt from its initial orientation. Finally, at much larger applied electric field strength refereed to saturation field, all molecules orients along external electric field direction. Therefore, through transition from Frederiks to the saturation field.

3. Results and discussion

In this section, results obtained with our numerical procedure will be discussed. Then, we will compare our results with previous works. We suppose our ferronematic system contains 5CB NLC which has been doped with $Sn_2P_2S_6$ NPs. We use experimental data listed in Table 1.

Table 1. Experimental data used for 5CB NLC and $Sn_2P_2S_6$ nanoparticles.[48,49]

Parameter	Value	Description
K_1	10.5×10^{-12} N	splay elastic module
K_2	5.4×10^{-12} N	twist elastic module
K_3	13.8×10^{-12} N	bend elastic module
ε_a	11.5	nematic dielectric anisotropy
$\varepsilon_\perp$	7	normal component of NLC electric permittivity

By using our numerical technique we compute Frederiks threshold field for different concentration of volume fractions under various anchoring strengths to present the effects of anchoring condition on different volume fractions. Finding results are illustrated in Fig. 3. It shows that increasing the percent of doped ferroelectric NPs results in decreasing the threshold field in all of various anchoring strength. An interesting thing is that rate of decreasing is equal to all of these anchoring strength. Ferroelectric NPs due to their polarization induce an electric field which interacts with NLC molecules and results in lower Frederiks threshold. As it is shown in Fig. 3, under stronger anchoring condition, molecules are kept a tight hold on the substrates and hence, the Frederiks transition happens in larger values. The phase diagram of NP permanent polarization as a function of electric Frederiks threshold field is illustrated in Fig. 4. It is obvious to see that threshold field decreases when the NP polarization is increased. A

similar results are seen in Fig. 3. However, a striking feature of Fig. 3 is to happen saturation when permanent polarization, d is reduced. There is nothing happened in the assumed ferronematic system below Frederiks transition. Nevertheless, above Frederiks transition, all molecules rotate to the applied electric field direction. As the external $\boldsymbol{E}$ is larger, molecules will be more aligned.

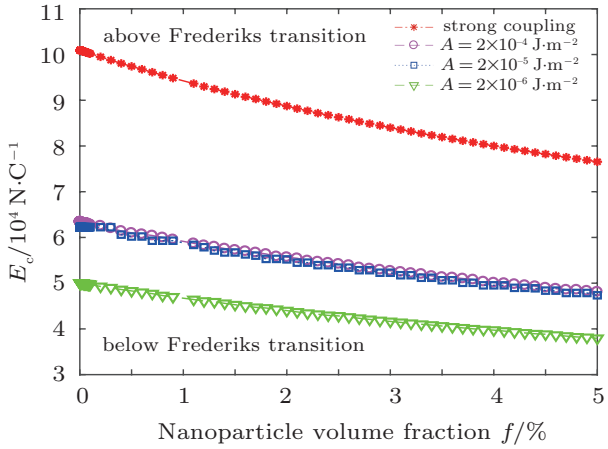


Fig. 3. (color online) Phase diagram for NPs volume fraction as a function of Frederiks threshold field and permanent polarization $d = 0.06$ C $\cdot$ m^{-2}, volume size $v = 1\times10^{-25}$ m^3, and cell thickness $L = 10$ µm. As the anchoring strength decreases, Frederiks transition takes place in lower values and molecules weakly anchored to the substrates rotate more easily. The reduction in the Frederiks threshold field is linear for various anchoring condition (see the text for details).

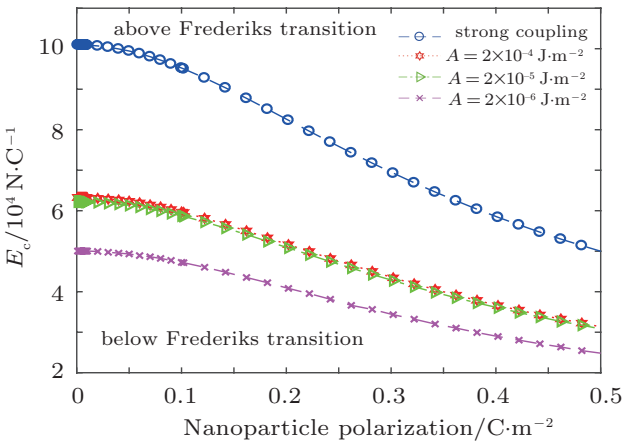


Fig. 4. (color online) Phase diagram for NPs permanent polarization as a function of Frederiks threshold field and NP volume fraction $f = 0.3\%$, volume size $v = 1\times10^{-25}$ m^3, and cell thickness $L = 10$ µm. NPs polarization induce an electric field which interacts with the system and reduces threshold field. Stronger anchoring conditions lead to the larger threshold field. However, as the permanent polarization decreases, increasing in the threshold field leads to the saturation for all of anchoring conditions (see the text for details).

There are other parameters which can be manipulated to get more optimized Frederiks threshold field, for example, NP size and cell thickness. Figure 5 presents the influence of radius on the transition threshold field in different anchoring condition. It is clear that the effect of NP size is more or less similar to its permanent polarization. When smaller NP radius is used, this leads the Frederiks threshold field to the saturation, which we have seen before in Fig. 4 through investigating the effects of NP permanent polarization. On the other hand, there is smaller applied electric field is need to take place the Frederiks transition with larger NPs size. It means that larger NP radius can affect and cover more area and thus interact with more NLC molecules. Nevertheless, too large NP radius can totally disturb the NLC properties. Generally, it will be reasonable to expect that the effects of colloidal size is the same as its permanent polarization in a suspension containing many colloidal particles.

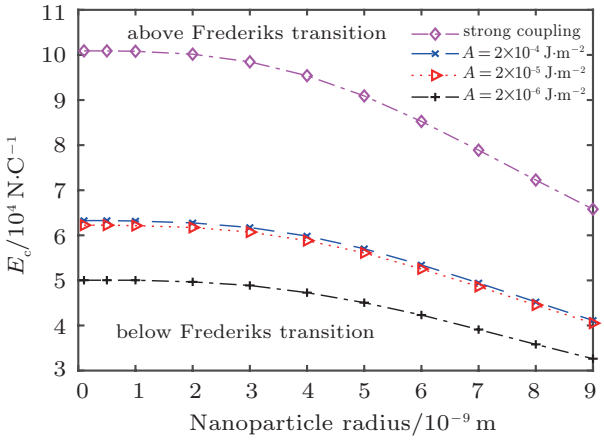


Fig. 5. (color online) The influence of colloidal radius on the Frederiks threshold field in different anchoring conditions. There is not a linear dependency on the Frederiks threshold field and NP radius. Decreasing the NP radius leads the threshold field to the saturation. While, colloids with larger radius induce electric field which covers more NLC molecules and hence results in lower threshold field. Numerical data: $d = 0.06$ C $\cdot$ m^{-2}, $f = 0.3\%$, and $L = 10$ µm.

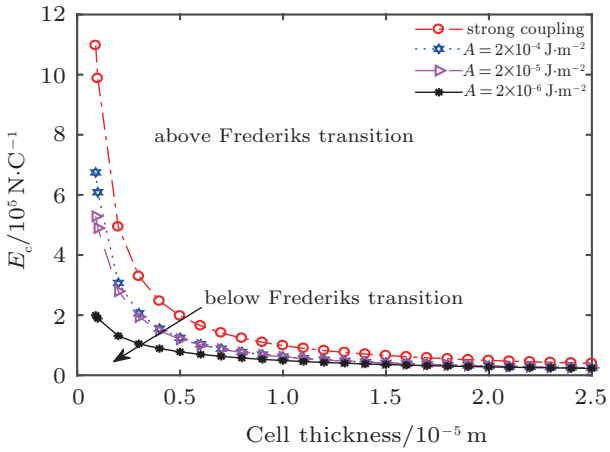


Fig. 6. (color online) Effects of cell thickness on the Frederiks transition in different anchoring condition. Frederiks transition can be sophisticated controlled by adjusting the cell thickness because of its high impact in comparison to the other control parameters. As cell thickness gets much thicker, falling in threshold field becomes more steep. On the other hand, there is larger applied electric field is needed For the Frederiks transition in thin ferronematic cells. Numerical data: $d = 0.06$ C $\cdot$ m^{-2}, $f = 0.3\%$, and $v = 1\times10^{-25}$ m^3.

Figure 6 illustrates phase diagram of electric Frederiks transition as a function of cell thickness. Thinner ferronematic cells need larger applied electric field to reach to the Frederiks

transition. For thicker cells, falling in threshold field becomes more steep. However, anchoring strength will be less important as the cell thickness gets thicker. It is obviously clear that the cell thickness parameter has higher impact on the Frederiks transition threshold in comparison to the anchoring condition.

Anchoring strength determines how NLC molecules tightly bind into the substrates. Adjusting the anchoring strength can be done technically by adding the surfactant to the system. Different anchoring strengths cause different values of pre-tilt angles, θ_0, and behavior of NLC molecules at the nematic–wall interfaces. In the case no anchoring condition, $A = 0$, equation (7) yields $\mathrm{d}\theta/\mathrm{d}z = 0$ and thus it is revealed from graphical solution of Fig. 2 that θ is $\pi/2$ at the boundary surfaces. Namely, under the condition of $A = 0$, current homogeneous anchoring condition changes to the homeotropic ones under the influence of external electric field in the z direction. Moreover, the transition from Frederiks to the saturation region occurs sharply and by the way all molecules within the cell are rapidly aligned to $\boldsymbol{E}$ under the influence of electric threshold field (see Fig. 7). This sharp transition is so-called the spontaneous Frederiks transition.[50]

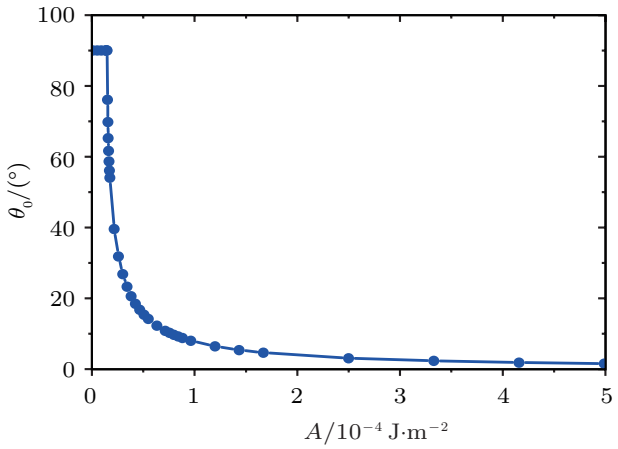


Fig. 7. (color online) Dependency of anchoring strength as a function of θ at the boundary surfaces, θ_0. Numerical data: $E = 4 \times 10^5$ N $\cdot$ C^{-1}, $d = 0.06$ C $\cdot$ m^{-2}, $f = 0.3\%$, $\nu = 1 \times 10^{-25}$ m^3, and $L = 10$ μm.

From Fig. 7, under the condition of huge anchoring strength, $A \to \infty$, θ_0 reaches to zero and homogeneous anchoring condition does not changed here. By this way, Frederiks transition occurs at higher values of applied electric field when there are larger anchoring strengths are established. Generally, electric Frederiks threshold field has a dependency on the anchoring strength, NP permanent polarization, NP volume fraction, NP radius and cell thickness. It is also interesting to examine how the Frederiks threshold field changes under the influence of different anchoring strength. Figure 8 presents anchoring strength as a function of electric threshold field. From low anchoring strength to $A = 0.1 \times 10^{-3}$ J $\cdot$ m^{-2}, increasing in E_c becomes more steep. Nevertheless, we will reach a plateau after this value.

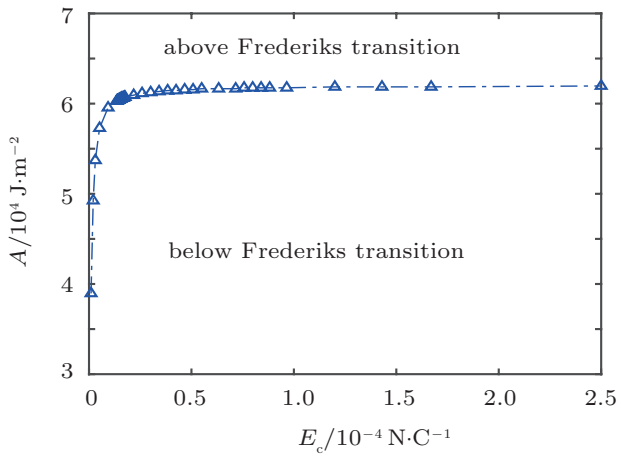


Fig. 8. (color online) Phase diagram of anchoring strength as a function of electric threshold field (see the text for details). $d = 0.06$ C $\cdot$ m^{-2}, $f = 0.3\%$, $\nu = 1 \times 10^{-25}$ m^3, and $L = 10$ μm.

3.1. Validation

Here, we validate our numerical results by comparing them with previous works. In this work, we have investigated the influence of different parameters on the electric Frederiks threshold field, for example, NP radius, polarization, volume fraction, anchoring strength and cell thickness. At large NP polarization, radius or volume fraction, the results may not be accurate due to the aggregation phenomenon. Aggregation is more probable to happen in the center of slab since the NLC director is most free to rotate toward the external field.[51] In this case NLC properties are locally perturbed, electric filed is not uniform within the cell and order parameter is needed to be taken into account. Our findings are consistent with Podoliak[18] whose studying reports that reduction in Frederiks threshold field is proportional to the NP concentration and polarization. They have also predicted that different shapes of NP have discernible Frederiks transition. Napoli[52] established Euler–Lagrangian equation for the total free energy and used a regular perturbation method to find the equilibrium solution. He has categorized the solution into two distinct regions, Frederiks and saturation regions. It has been reported the effects of two different anchoring energies at critical field and high applied voltages. Burylov and Raikher[17] have governed initial continuum theory[13] to study anchoring energy of NLC molecules at the ferroparticles. Anchoring of NLC molecules at the substrates and also at the ferroparticles surfaces have taken into account by Zadorozhnii[51] to investigate the magnetic Frederiks transition in the ferronematic systems. In the current work, However, we have used Euler-Lagrangian equation together with relaxation method and Maxwell construction to tackle with the difficulties arisen out of difficult boundary condition and select the physically acceptable solutions.

4. Conclusions

The effect of anchoring strength, nanoparticle volume fraction, nanoparticle size, permanent polarization, and cell thickness on the Frederiks threshold field in a nematic liquid crystal doped with ferroelectric colloidal nanoparticles in weak anchoring condition have been numerically studied. A low concentration of ferroelectric nanoparticles were assumed to avoid totally disturbance the system. A phenomenological formula provided by Rapini–Papoular was used to explain the NLC anchoring at the substrates. Using the relaxation method and Maxwell construction, we have numerically solved the Euler–Lagrangian differential equation for the ferronematic total free energy together with the surface energy to obtain the equilibrium states of the NLC director within the slab. We have focused our attention to calculate the phase diagrams for nanoparticle volume fraction, nanopaticles size, permanent polarization, and cell thickness as a function of anchoring strength which have been not investigated in our previous work. Numerical results indicate that larger NP radius or larger permanent polarization or volume fraction result in producing an stronger induced electric field which causes Frederiks transition to take place at lower threshold field. The behavior of permanent polarization and NP radius are nearly similar and both of them lead the Frederiks field to the saturation as a result of decreasing in these parameters. However, this situation does not happen for nanoparticle volume fraction. Dependency of cell thickness on the threshold field reveals that Frederiks transition takes place at larger external electric fields for more compact cells. However, the threshold field falls into lower values as a result of increasing in cell thickness and thus anchoring strength gradually looses its impact on the threshold field. Moreover, when the cell thickness is fixed, there is also a plateau region for the anchoring strength reaching 6×10^4 J $\cdot$ m^{-2} and molecules rapidly orient to the applied electric field.

Acknowledgment

One of the authos (EK) acknowledges the support of Shiraz University of Technology Research Council.

References

[1] Efron U 1995 *Spatial Light Modulator Technology: Materials, Devices, and Applications* (Dekker)
[2] Bortolozzo U, Clerc M G, Falcon C, Residori S and Rojas R 2006 *Phys. Rev. Lett.* **96** 214501
[3] Residori S, Bortolozzo U, Huignard J P 2008 *Phys. Rev. Lett.* **100** 203603
[4] MÍnguez-Vega G, Supradeepa V R, Mendoza-Yero O and Weiner A M 2010 *Opt. Lett.* **35** 2406
[5] Alberucci A, Piccardi A, Bortolozzo U, Residori S and Assanto G 2010 *Opt. Lett.* **35** 390
[6] Maurer C, Jesacher A, Bernet S and Ritsch-Marte M 2011 *Laser Photon. Rev.* **5** 81
[7] Kaczmarek M and Dyadyusha A 2004 *J. Appl. Phys.* **96** 2616
[8] Cook G, Glushchenko A V, Reshetnyak V Yu, Beckel, E R, Saleh M A and Evans D R 2008 *IEEE/LEOS Winter Topical Meeting Series*, January 14–16, 2008, Sorrento, Italy, p. 129
[9] Cook G, Glushchenko A V, Reshetnyak V, Griffith A T, Saleh M A and Evans D R 2008 *Opt. Express* **16** 4015
[10] Khoo I C 2007 *Liquid crystals*, 2nd edn. (New Jersey: John Wiley and Sons)
[11] Beeckman J, Neyts K and Vanbrabant P J M 2011 *Opt. Eng.* **50** 081202
[12] Bahadur B 1990 *Liquid Crystals Applications and Uses*, Vol. 3 (Toronto: World Scientific)
[13] Brochard F and de Gennes P G 1970 *J. Phys.* **31** 691
[14] Burylov S V and Raikher Y L 1994 *Phys. Rev. E* **50** 358
[15] Raikher Yu L, Burylov S V and Zakhlevnykh A N 1987 *J. Magn. Magn. Mater.* **65** 173
[16] Raikher Y L and Stepanov V I 1999 *J. Magn. Magn. Mater.* **201** 182
[17] Burylov S V and Raikher Y L 1995 *Mol. Cryst. Liq. Cryst.* **258** 123
[18] Podoliak N, Buchnev O, DÁlessandro G, Kaczmarek M, Reznikov Y and Sluckin T J 2011 *Soft Matter* **7** 4742
[19] Dierking I, Scalia G and Morales P 2005 *J. Appl. Phys.* **97** 44309
[20] Al-Zangana S, Turner M and Dierking I 2017 *J. Appl. Phys.* **121** 085105
[21] Stark H 2001 *Phys. Rep.* **351** 387
[22] Smalyukh I I, Lavrentovich O D, Kuzmin A N, Kachynski A V and Prasad P N 2005 *Phys. Rev. Lett.* **95** 157801
[23] Yada M, Yamamoto J and Yokoyama H 2004 *Phys. Rev. Lett.* **92** 185501
[24] Poulin P, Stark H, Lubensky T C and Weitz D A 1997 *Science* **275** 1770
[25] Gu Y and Abbott N L 2000 *Phys. Rev. Lett.* **85** 4719
[26] Musevic I, Skarabot M, Tkalec U, Ravnik M and Zumer S 2006 *Science* **313** 954
[27] Hakobyan M R, Alaverdyan R B, Hakobyan R S and Chilingaryan Yu S 2014 *Armen. J. Phys.* **7** 11
[28] Reznikov Y, Buchnev O, Tereshchenko O, Reshetnyak V, Glushchenko A and West J 2003 *Appl. Phys. Lett.* **82** 1917
[29] Ouskova E, Buchnev O, Reshetnyak V, Reznikov Y and Kresse H 2003 *Liq. Cryst.* **30** 1235
[30] Bing G Y, Hai C Y, Ying X, Chun Q S and Zhan-Guo W 2011 *Chin. Phys. Lett.* **28** 096101
[31] Lopatina L M and Selinger J V 2009 *Phys. Rev. Lett.* **102** 197802
[32] Lopatina L M and Selinger J V 2011 *Phys. Rev. E.* **84** 041703
[33] Mukherjee P K 2017 *J. Mol. Liq.* **225** 462
[34] Mukherjee P K 2016 *Europhys. Lett.* **114** 56002
[35] Uchida T and Seki H 1992 *In Liquid crystals: Applications and Uses*, ed. Bahadur B, Vol. 3 (Singapore: World Scientific) p. 63
[36] Ge J J, Li C Y, Xue G, Mann I K, et al. 2001 *J. Am. Chem. Soc.* **123** 5768
[37] Toney M F, Russell T P, Logan J A, Kikuchi H, Sands J M and Kumar S K 1995 *Nature* **374** 709
[38] Yaroshchuk O and Reznikov Y 2012 *J. Mater. Chem.* **22** 286
[39] Rong-Hua G 2012 *Acta Phys. Sin.* **61** 156102
[40] Kadivar E, Bahr C and Stark H 2007 *Phys. Rev. E* **75** 061711
[41] Ying Z M, Merlitza H and Xua W C 2015 *Chin. Phys. B* **24** 026101
[42] Evans S D, Allinson H, Boden N, Flynn T M and Henderson J R 1997 *J. Phys. Chem. B* **101** 2143
[43] Ramdane O O, Auroy P, Forget S, Raspaud E, Martinot-Lagarde P and Dozov I 2000 *Phys. Rev. Lett.* **84** 3871
[44] Ruetschi M, Grutter J, Funfschilling J and Gunterodt H J 1994 *Science* **265** 512
[45] Farrokhbin M and Kadivar E 2016 *Physica A* **462** 725
[46] Rapini A and Papoular M 1969 *J. Phys.* (Paris) **30** 54
[47] Kadivar E 2009 *Phys. Rev. E* **80** 011701
[48] Shelestiuk S M, Reshetnyak V Y and Sluckin T J 2011 *Phys. Rev. E* **83** 041705
[49] Basu R and Iannacchione G S 2009 *Appl. Phys. Lett.* **95** 173113
[50] Blinov L M and Chigrinov V G 1994 *Electrooptic Effects in Liquid Crystal Materials* (New York: Springer)
[51] Zadorozhnii V I, Sluckin T J, Reshetnyak V Y and Thomas K S 2008 *SIAM J. Appl. Math.* **68** 1688
[52] Napoli G 2006 *J. Phys. A: Math. Gen.* **39** 11